IEEE Access
Multidisciplinary ⋮ Rapid Review ⋮ Open Access Journal

Received March 17, 2022, accepted April 11, 2022, date of publication April 18, 2022, date of current version April 26, 2022.

Digital Object Identifier 10.1109/ACCESS.2022.3167701

Inrush Current Management During Medium Voltage Microgrid Black Start With Battery Energy Storage System

MAHDI SHAHPARASTI[1], (Senior Member, IEEE), HANNU LAAKSONEN[1], (Member, IEEE), KIMMO KAUHANIEMI[1], (Member, IEEE), PANU LAUTTAMUS[2], STEFAN STRANDBERG[2], AND JAN STRANDBERG[3]

[1]School of Technology and Innovations, University of Vaasa, 65200 Vaasa, Finland
[2]Danfoss Drives, 65380 Vaasa, Finland
[3]Caruna, 02600 Espoo, Finland

Corresponding author: Mahdi Shahparasti (mahdi.shahparasti@uwasa.fi)

This work was supported by the Business Finland through the SolarX Research Project, in 2019–2021, under Grant 6844/31/2018.

ABSTRACT This paper addresses the black start of medium voltage distribution networks (MV-DNs) by a battery energy storage system (BESS). The BESS consists of a two-level voltage source inverter interfacing MV-DN which has limited overcurrent capability. On the other hand, MV-DN normally includes several step-up and step-down transformers that are drawing sympathetic inrush current in energizing stage. Therefore, the major difficulty to perform black start by BESS during MV-DN island operation lies in the fact that the inverter has to simultaneous control the network voltage and its output current. This paper presents two control approaches for a BESS in order to control the inrush current during MV-DN black start. The proposed control schemes consist of droop, voltage and current loops in the stationary reference frame. The droop loop is used to generate the voltage reference. An intermediate voltage and inner current loops are designed for output voltage regulation, current reference generation as well as current tracking, respectively. New reference modifiers are included into droop and voltage loops to limit inrush current. The proposed control schemes are experimentally tested for energizing Ingå MV-DN in Finland by 1 MVA BESS, and their performance is compared in terms of inrush current value and voltage quality. The obtained results prove that both methods are able to feed the load with a fixed voltage in the steady-state as well as to limit the transformer inrush current considering the inverter overcurrent limit.

INDEX TERMS Black start, distribution network, battery energy storage system, grid-forming, islanded mode, inrush current, medium voltage, microgrid.

NOMENCLATURE

2L-VSI	two level voltage source inverter
B	flux density
B_m	maximum flux density of transformer
B_s	the flux density of saturated core
B_r	residual flux density
BESS	Battery energy storage system
C_f	capacitor of LCL filter
CB	circuit breaker
DSO	distribution system operator
f_o	nominal frequency in Hz
f_s	switching frequency of converter
i, i_o	current of the converter and the grid
k_c	current controller gain
k_p	proportional gain
k_i	resonant gain
m, n	droop coefficients
L_f	converter side inductor of LCL filter
L_g	grid side inductor of LC filter
LV	low voltage
MV-DN	medium voltage distribution network
$G_i(s)$	current controller
$G_v(s)$	voltage controller
PCC	point of common coupling

The associate editor coordinating the review of this manuscript and approving it for publication was N. Prabaharan.

P, Q	exchanged active and reactive power with the grid
PI	Proportional Integral
PR	proportional resonant
r_f, r_g	internal resistance of L_f, L_g
SVM	Space Vector Pulse Width Modulation
s	Laplace operator
V_{DC}	DC bus voltage
V_i	output voltage of converter
V	PCC voltage
$\|V\|$	voltage amplitude
Z_g	equivalent grid impedance
$T_i(s)$	Transfer function between PCC voltage and converter voltage
$Z_o(s)$	equivalent impedance of the converter
Z_v	virtual impedance transfer function
$\Delta_p(s)$	characteristic equation
ω_o	resonant frequency PR controller in rad/s
Z and θ	the magnitude and phase of the connection line impedance

SUBSCRIPTS AND SUPERSCRIPTS

a,b,c	phase
i	converter
max	maximum
nom	nominal
DC	DC link
α, β	Stationary reference frame components
d, q	synchronous reference frame components
$*$	reference

I. INTRODUCTION

The black start of the distribution system is vital to feed medium voltage and low voltage customers with minimum elapsed time between inherent outages and to reduce mean time between failures (MTBF). There are two ways to perform black start. The first method recommends using a large installed generation, typically connected to the sub-transmission network, in order to self-start and re-energize the network [1]. The second requires the establishing and operation of small self-contained distribution-level microgrids or power islands at medium voltage (MV) levels [2]. The dispatchable distributed generation for instance diesel generators and battery energy storage systems (BESSs) as well as non-dispatchable generation such as small wind farms and commercial and industrial PV systems generation sources are envisaged to form the grid in islanded microgrids [2]. The size of the power islands is foreseen to be tens of MWs and will typically consist of one or more medium voltage feeders at a distribution network [3].

In the black start by BESS, the control scheme of the inverter plays an important role in forming medium voltage distribution networks (MV-DN) voltage, and BESS is forced to act like an AC voltage source [4], [5]. In the case of MV-DN, the voltage must be kept sinusoidal with limited voltage total harmonic distortion (THD), acceptable voltage deviation, balanced and fast transient voltage recovery under unpredictable load changes [6], [7]. Other disturbances during the black start and forming of the MV-DN voltage can be related to the inherent nonlinearities of the inverter and the dc-bus voltage fluctuations due to battery discharge [4]. In general, two different control methods can be used for an inverter with grid-forming capability: 1) constant voltage method and 2) droop method.

In the constant voltage method, the inverter output always keeps constant regardless of load changes. This method works correctly when other generating units are operating as current sources, and using wire communications is mandatory for power-sharing [8]. In droop control, the voltage amplitude and frequency are reduced when load active and reactive power increases. This method is suitable for a system with several static and spinning generators in parallel wherein power-sharing will be realized without any communication lines among them [9].

For the implementation of both control strategies, cascaded voltage and current loops are mainly utilized in which the voltage controller in charge to track the reference of voltage and the current controller is used to improve system stability and protection. A variety of controllers such as classic proportional-integral (PI) and proportional resonant (PR) controllers as well as nonlinear controllers including deadbeat [10], sliding mode [11] and model predictive controllers [12] have been proposed as voltage and current controllers. Nonlinear controllers are either still highly dependent on the correctness of the parameters or safer from the chattering problem. Therefore, classical PI and PR controllers in synchronous and stationary reference frames have their place in the industry despite of their limitations in the compensation of all harmonics[13]. In contrast to the constant voltage method, the droop control method is superior to control BESS in microgrids and distribution systems with several resources since it offers wireless and flexible power-sharing [14], [15].

The transformer's magnetization current generated at the energizing moment is known as an inrush current which can exceed ten times the nominal current of a transformer for 4–6 cycles [16]. In a system, like MV-DN, with several transformers in series and parallel, another phenomenon entitled sympathetic inrush might occur due to the switching of one transformer while other transformers are previously energized. The peak of the inrush current is higher than the sympathetic inrush current; however, the inrush current usually decays in a few cycles while the sympathetic inrush current can continue for seconds [17]. So far, transformers of MV-DN have been considered ideal in the design and implementation of the control scheme of inverter-based generating units. Therefore, BESS with a regular controller cannot perform black start in real MV-DN due to overcurrent trip caused by inrush and sympathetic inrush currents of

transformers. Some efforts to limit inrush phenomena were done in [18], [19] by closing the circuit breaker (CB) at the optimum time but is not working for MV-DN because the circuit breakers are switched by the distribution system operator (DSO) and also there is no knowledge about parameters of transformers.

In this paper, new control schemes are proposed to reduce inrush currents and perform black start in MV-DN. These methods are developed without the need for any information about transformer parameters, core saturation curve and residual flux, and timing of CBs. Therefore, the proposed new schemes provide improved and effective performance, reduced calculation time burden, uncomplicated implementation, and independence from the distribution network protection and management system.

This paper is arranged as follows. In Section II, the configuration of the medium voltage BESS is described. Section III provides the development of the proposed controllers and the experimental results of black starting of Ingå MV-DN by 1 MVA BESS will be addressed in Section IV. The conclusions of the work are presented in Section V.

II. MEDIUM VOLTAGE BESS CONFIGURATION

A. SYSTEM CONFIGURATION

In available BESS systems, BESS voltage is typically lower than 1500 V on the DC side. Therefore, one DC/AC converter (inverter) plus a step-up transformer is used to connect BESS into the AC grid. For the inverter mainly a 2-level voltage source inverter (2L-VSI) technology with an LCL filter on the AC side is applied. The VSI technology has many technical advantages, including commutation failure robustness, supplementary services, reactive power control and consequently voltage control [20]. The nominal AC voltage of the inverter terminal is typically in the range of 380 V to 690 V. Therefore, using a step-up transformer is mandatory for connecting BESS to the MV grid. A single line diagram of an MV distribution network including BESS is shown in Fig. 1, where a CB is responsible for connecting and disconnecting BESS. The CB is controlled by the DSO and the BESS controller does not have any control and information about CB's timing and technical parameters. Depending on the needed power of loads in the grid, several 2L-VSIs will operate in parallel. They will connect to the same DC link on the BESS side (see Fig. 1). On the grid-side, 2L-VSIs are connected in parallel after LCL filters (see Fig. 1). The nominal current of semiconductors of 2L-VSI will be selected slightly larger than the maximum load current because semiconductors do not have the overload current carrying capability, and converters will trip if the current exceeds this value [21].

There are several challenges to control BESS in the MV grid due to step-down and step-up transformers. One of them is the sympathetic inrush current of transformers, since inrush currents can be several times higher than nominal currents of transformers, and 2L-VSI cannot provide this current during islanded distribution network section black start and when forming a grid.

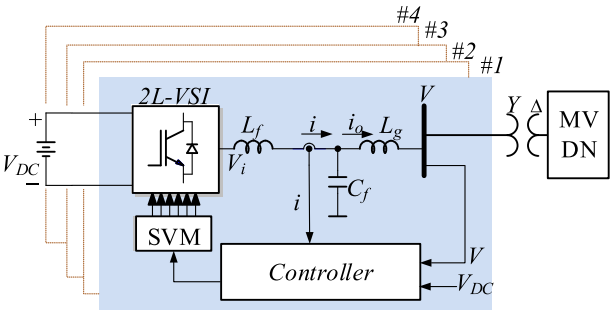

FIGURE 1. The circuit diagram of MV BESS.

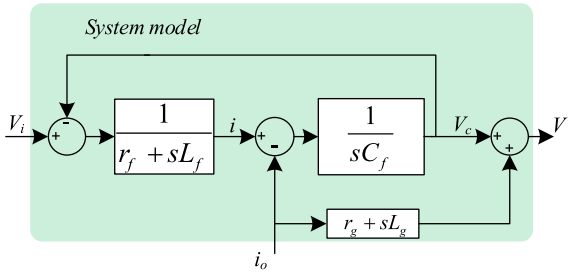

FIGURE 2. Model of an inverter with LCL filter in the grid-forming mode.

B. SYSTEM MODEL

The dynamic model of an inverter with an LCL filter in grid-forming mode is shown in Fig. 2 which can be mathematically described by the following transfer functions [22]:

$$V(s) = T_i(s)V_i(s) + Z_o(s)i_o(s), \tag{1}$$

$$T_i(s) = \frac{1}{\Delta_p(s)}, \tag{2}$$

$$Z_o(s) = \frac{-s^2 L_f L_g + s\left(L_g(1-r_f) - r_g L_f\right) + r_g(1-r_f)}{\Delta_p(s)}, \tag{3}$$

where the denominator $\Delta_p(s)$ can be expressed as:

$$\Delta_p(s) = s^2 L_f C_f + sC_f r_f + 1, \tag{4}$$

and $V_i(s)$, $i_o(s)$ and $V(s)$ are the inverter output voltage, the output current, the point of common coupling (PCC) voltage, respectively. In this system, V_i and i_o are accounted as the control input and the disturbance, respectively. The voltage of PCC V is the output of this system.

In this system, i_o as the output current of the inverter mainly includes MV-DN loads currents in the steady-state which can be either linear or nonlinear with acceptable changes depending on the nature of loads. However, inrush and sympathetic inrush currents will flow in the case of energizing transformers for several cycles. The inrush current of a transformer can be expressed as follows (see Fig. 3 [18]):

$$i_{inrush} = -\frac{V_p X}{Z^2}\left(\begin{array}{l}\frac{R}{X}\sin(\omega t) - \cos(\omega t) \\ +e^{-\frac{R(\omega t+\theta)}{X}}\left(\frac{R}{X}\sin(\theta) - \cos(\theta)\right)\end{array}\right), \tag{5}$$

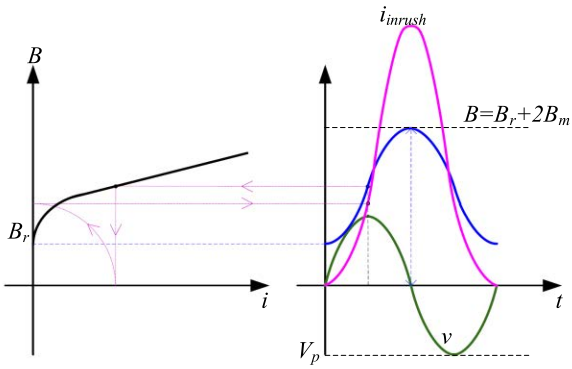

FIGURE 3. Magnetization curve and inrush current waveforms.

where V_p is the peak of the applied voltage, ω is the grid frequency, $X = X_o + X_T$ is the inverter and transformer reactance, $R = R_o + R_T$ is the inverter and transformer winding resistance, $Z = Z_o + Z_T$ is the inverter and transformer impedance. Subscripts o and T remark the inverter and the transformer. The angle θ_T is described by the following relationship [23], [24]:

$$\theta_T = \cos^{-1}\left(\frac{B_s - B_r - B_m}{B_m}\right), \tag{6}$$

where B_m is the maximum flux density of transformer excited by the rated voltage, B_s is the flux density of the completely saturated core, and B_r is residual flux density. According to (6), there are two ways to limit inrush current: 1) choosing the best time for connection, which is not applicable in this application since CB is controlled by DSO, and 2) reducing the voltage amplitude, which is feasible and can be implemented by the control scheme of the BESS inverter.

III. CONTROL SCHEME OF MV BESS WITH BLACK START CAPABILITY

A. CONTROL LOOPS

The proposed BESS inverter control schemes as shown in Fig. 4 include outer and inner loops, to reach zero steady-state error and fast transient response with a satisfactory stability margin. The way to control inrush current is the key difference of control schemes which will be discussed in incoming sections.

The envisioned control scheme is realised in the stationary reference frame to omit coordinate transformations. Alternatively, the control scheme could be implemented in the rotating (synchronous) reference frame. The voltage loop is employed to guarantee steady-state reference tracking performance and the inner loop provides damping for unstable dynamics and rapid compensation of system disturbances such as step loads and reference changes. In the next subsections, the development of current and voltage loops will be discussed based on the control block diagram of MV BESS in Fig. 5 [19].

The current loop's block diagram can be simplified as Fig. 6. For better circuit resonance damping and inverter protection, the inductor current is employed in the current loop [16]. The plant transfer function is given by (7) wherein the disturbance input (i_o) is ignored.

$$\frac{i(s)}{V_i(s)} = \frac{sC_f}{1 + s^2 L_f C_f}, \tag{7}$$

where inductor current and inverter output voltage are represented by i and V_i, respectively. This system has a low level of stability and is prone to resonant oscillation. The closed-loop transfer function can be obtained by utilizing a a proportional controller in the current loop ($G_i(s) = k_c$).

$$\frac{i(s)}{i^*(s)} = \frac{sk_cC_f}{1 + sk_cC_f + s^2 L_f C_f}. \tag{8}$$

It is obvious that increasing the current controller gain (k_c) will result in greater resonant oscillation damping and faster tracking of the reference current. On the other hand, bigger k_c leads to the development of high-order harmonics and instability [20].

The choice of current controller gain (k_c) is, in fact, a trade-off between tracking error and stability. The value of k_c must be within the following range:

$$\sqrt{\frac{4L_f}{C_f}} \le k_c \le 12 f_s L_f. \tag{9}$$

When a nonlinear load is fed by MV BESS, such as a rectifier and transformers, the output voltage contains harmonics other than the fundamental. As a result, limiting voltage distortion in supplying nonlinear loads becomes a difficult problem, prompting the development of a range of control approaches. Conventional multi-loop PI controllers in the synchronous reference frame can be used to reject the disruptive influence of load current on the output voltage, as shown in Fig. 7. The effectiveness of this method is not restricted by switching frequency, unlike many other methods such as deadbeat, feedback linearization method, and sliding-mode control. This approach, however, is commonly criticized for the restricted number of harmonics it can compensate. This is owing to the computational difficulty and computational weight of the coordinate transformations required for synchronous frame implementation [13]. In this method, output voltage regulation is achieved by sensing the output voltage and comparing it to the reference voltage, as shown in Fig. 7. The error signal in the stationary frame is converted to the synchronous reference frame with a rotational speed of $k\omega$, where k is one, three, five, and so on. The PI controller processes the error in the synchronous frame and converts it to the stationary frame current reference signal $i^*_{\alpha\beta}$.

The voltage loop is slower than the current loop. As a result, the gain of the current loop can be assumed to be one when designing the voltage controller. Fig. 7 displays the model of a PI harmonic controller in harmonic frame k. The following expression is the result of converting one control channel of Fig. 7 from the synchronous frame with of speed

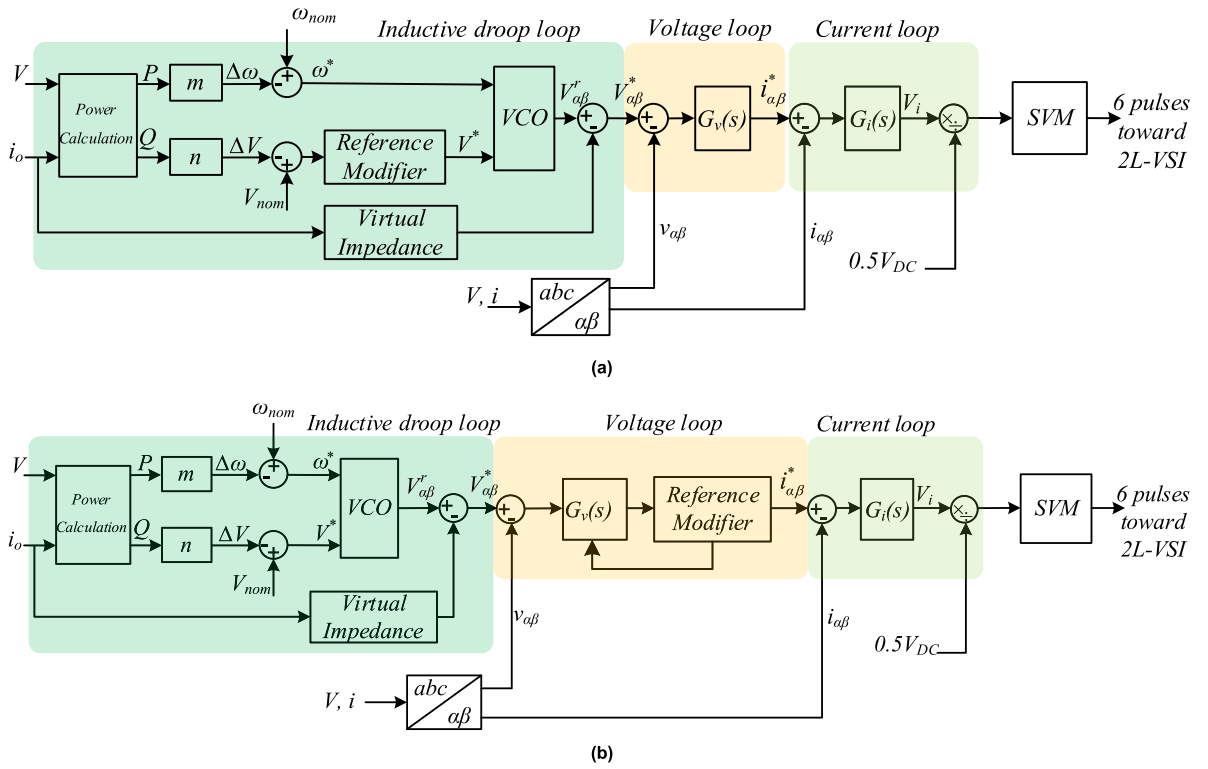

FIGURE 4. Modular framework for controlling MV BESS: (a) Control method based on reference limiter in droop loop, (b) Control scheme based on reference limiter in voltage loop.

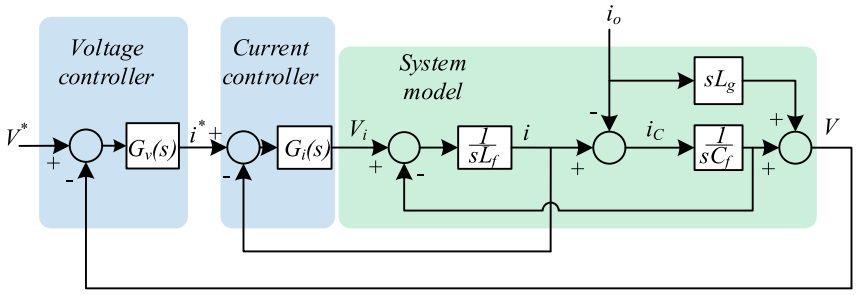

FIGURE 5. System model and control block diagram of MV BESS.

$k\omega$ to the stationary reference frame:

$$\begin{bmatrix} i^*_{\alpha k} \\ i^*_{\beta k} \end{bmatrix} = \begin{bmatrix} k_p + \dfrac{k_{ik}s}{s^2 + k^2\omega_o^2} & 0 \\ 0 & k_p + \dfrac{k_{ik}s}{s^2 + k^2\omega_o^2} \end{bmatrix} \cdot \begin{bmatrix} \Delta v_\alpha \\ \Delta v_\beta \end{bmatrix}, \tag{10}$$

The gains of proportional and integral controllers in reference frame k are denoted by k_p and k_{ik}, respectively. In addition, ω_o represents the fundamental angular frequency in rad/sec. Consequently, the multi-loop control with PR controllers in the voltage loop is shown in Fig. 8. PR controller can be expressed as follows[25]:

$$G_v(s) = K_p + \sum_{k=1,3,5,7} \frac{K_i}{s^2 + (k \times \omega_o)^2} \tag{11}$$

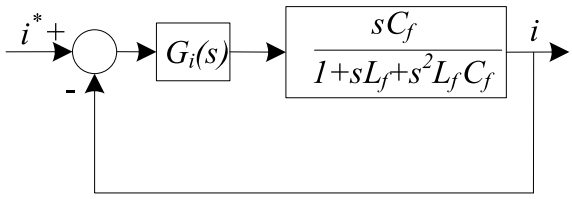

FIGURE 6. Inner current loop and plant transformer function.

In the above equation, if the voltage controller is assumed as two parts, the first part represents the proportional controller coefficient (K_p) and the second part is responsible for suppressing the resonance of the intended order ($i = 1, 3, 5$ & 7). So, i represents the harmonic order in K_i.

The droop strategy is a conventional method to generate the voltage reference based on active and reactive powers.

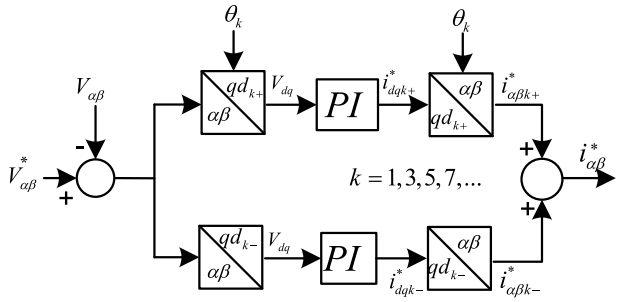

FIGURE 7. Multi-loop synchronous frame proportional-integral (PI) harmonic controller [13].

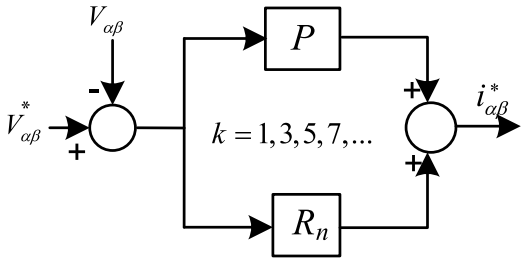

FIGURE 8. The block diagram of voltage loop with proportional-resonant controllers.

The principal concept of the droop method is to emulate the behaviour of a synchronous generator, which reduces the frequency, while the active power is increased. This feature can be utilized to perform communication-less power-sharing among parallel units. In the droop method, the inverter can be modelled as an ac source with the voltage amplitude of E and phase of δ. Then, the active and reactive powers of the inverter can be expressed as follows:

$$\begin{cases} P = \dfrac{V_{PCC}E}{Z}\cos(\theta-\delta) - \dfrac{V_{PCC}^2}{Z}\cos(\theta) \\ Q = \dfrac{V_{PCC}E}{Z}\sin(\theta-\delta) - \dfrac{V_{PCC}^2}{Z}\sin(\theta) \end{cases}, \quad (12)$$

where V_{PCC} is the voltage of the point of common coupling. Z and θ are the magnitude and phase of the connection line impedance. The phase θ is 0^o and 90^o for the inductive and resistive line impedance, respectively.

If the phase angle is small enough, then $\cos\delta \approx 1$ and $\sin\delta \approx \delta$. With this assumption, the active power mainly depends on the phase angle, while the reactive power essentially relies on the amplitude for the inductive line ($\theta = 90^o$). Accordingly, the voltage reference can be defined based on the droop method as follows for inductive line impedance:

$$\begin{cases} \omega^* = \omega_{nom} - mP \\ V^* = V_{nom} - nQ \end{cases}, \quad (13)$$

where ω^* refers to the reference frequency and V^* stands for the reference. Similarly, the voltage reference can be modified as follows for resistive line impedance:

$$\begin{cases} \omega^* = \omega_{nom} + nQ \\ V^* = V_{nom} - mP \end{cases}, \quad (14)$$

After the determination of references of the amplitude and the frequency, the voltage reference signal ($V^r_{\alpha\beta}$) is generated in the stationary reference frame by a voltage-controlled oscillator (VCO) as shown in Fig. 4.

Eqs (13) and (14) have been named as inductive (P-f/Q-V) and resistive (P-V/Q-f) droop methods, respectively, which both have their pros and cons. Thus, the type of droop strategy must be determined based on characteristics of MV-DN (cables, overhead lines, etc) and control schemes of other generating units in the system.

It is evident that active and reactive powers rely on Z and θ. In practice, the DN power system is not pure inductive or resistive, which has a negative impact on the accuracy of the droop method and power-sharing. As a solution, a virtual impedance can be employed to enforce the observed impedance by the inverter to be purely inductive or resistive [26]. After embedding the virtual impedance branch into the droop method in Fig. 4, the final voltage reference ($V^*_{\alpha\beta}$) can be expressed as:

$$V^*_{\alpha\beta} = V^r_{\alpha\beta} - Z_v.\, i_{o,\alpha\beta}, \quad (15)$$

where $i_{o,\alpha\beta}$ is the output current of the inverter, and Z_v is the virtual impedance transfer function [27].

B. INRUSH CURRENT LIMITATION

Two different types of reference modifiers can be employed in droop and voltage loops to limit inrush current depending on control loops.

1) B.1. REFERENCE MODIFIER IN DROOP LOOP

A rate limiter with the following relationship can be used as the reference modifier in the droop loop to restrict the pace of voltage amplitude and control the inrush current (see Fig. 4-a):

$$V^*(i) = \begin{cases} V^*(k-1) + R.T_s & V^*(k) \le V_{nom} \\ V_{nom} & else \end{cases}, \quad (16)$$

where k, V^*, R, T_s and V_{nom} are an integer, the amplitude of voltage reference, rising slew rate parameter, controller sample time, and nominal voltage, respectively.

2) B.2. REFERENCE MODIFIER IN VOLTAGE LOOP

A reference modifier, expressed in (17), can be added to the voltage loop to limit inrush current as shown in Fig. 4-b. The modifier activates if the inverter current would exceed the high current level I_{high} set above the inverter continuous capacity and below the protection levels. Upon the activation, the current reference is modified per (17) where I_{max} is temporarily reduced current limit which is recovered to normal once the current has returned below I_{high}. The level I_{max} is set

within the inverter's continuous current capacity to mitigate the inrush event and ensure uninterrupted operation[28].

$$i^*_{\alpha\beta} = \begin{cases} i^*_{\alpha\beta}, & \left|i^*_{\alpha\beta}\right| \le I_{high} \\ \dfrac{I_{\max}}{\left|i^*_{\alpha\beta}\right|} i^*_{\alpha\beta}, & \left|i^*_{\alpha\beta}\right| > I_{high} \end{cases}, \tag{17}$$

where $\left|i_{\alpha\beta}\right|$ and $\left|i^*_{\alpha\beta}\right|$ are vector magnitudes. When the output of the controller is inhibited by a limiter, any integrators within the controller may experience wind-up. Therefore, the voltage controller must have the anti-windup capability [29], [30].

IV. EXPERIMENTAL RESULTS

In order to test and validate the performance of the proposed control strategy under real conditions, a 1MVA BESS (shown in Fig. 9) is used to black start of MV distribution system in Ingå, Finland. This 20kV distribution system has around 400 customers and 30 distribution transformers (20kV/400V, sum of 2.5MVA). In these tests, a load of 250kW are connected to the 1MVA inverter and 1MWh Battery. 1MVA inverter system consisting of four parallel-connected inverter units.

The single line diagram of this grid is shown in Fig. 10, the grid is energized by closing the LV-circuit breaker. The step-up transformer is 1000 kVA, Dyn 11, 20500/410 V transformer. The DC link voltage varies around 650-800 VDC, and it depends on the battery state of charge. The parameters of the 2L-VSI of the BESS system is listed in Table 1. The control scheme uses inverter current, dc-link voltage, ac line voltage on the low voltage side as feedbacks to control the system.

The circuit breaker between the inverter and transformer is turned on and off by DSO, and its time of closing is random. 20kV/400V transformers are connected to the distribution system without any circuit breakers.

Two experimental cases have been selected in this validation stage, 1) black start with the voltage reference modifier in the droop loop, 2) black start with the current reference modifier in the voltage loop.

A. BLACK START WITH VOLTAGE REFERENCE MODIFIER IN THE DROOP LOOP

Supplying load with ramped voltage is the first solution for inrush current limitation as shown in Fig. 11. These data were recorded from the internal datalogger of one inverter. As can be seen, there is no overvoltage and under voltage in the voltage waveform, and the load is fed with a fixed voltage in terms of amplitude and frequency. On the other hand, the output current does not contain any overcurrent like the typical inrush current. It is worth mentioning that some DSOs do not prefer feeding loads with a ramped voltage, and they want to maintain the voltage in the normal operating range, e.g. between 0.90 pu and 1.05 pu, depending on the grid code [31].

FIGURE 9. 1 MVA Battery energy storage system installed in Ingå, Finland.

TABLE 1. Parameters of each inverter in 1MV BESS.

Symbol	Description	Value
V (V_{rms})	Nominal line voltage	400
I_{NOM} (A)	Rated current	460
V_{dc} (V)	Dc-link voltage	650-800
L_f (μH)	Inverter side inductor	146
C_f (μF)	Filter capacitor	120
L_g (μH)	Grid side inductor	73
f_O (Hz)	Rated frequency	50
f_S (kHz)	Switching frequency	3.6

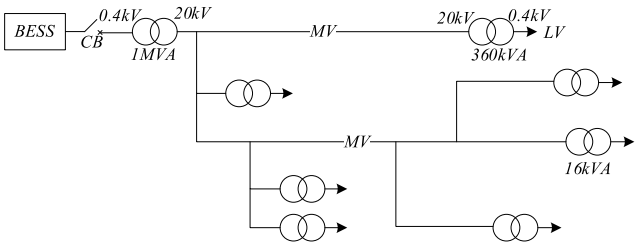

FIGURE 10. Single line diagram of the distribution system in Ingå, Finland.

B. BLACK START WITH THE CURRENT REFERENCE MODIFIER IN THE VOLTAGE LOOP

In the second experimental test, the performance of the proposed method with the current reference modifier in the voltage loop for instantaneous feeding of the load with nominal voltage as well as inrush current restriction will be evaluated.

In this test, the CB is closed in the LV side (400V) by the BESS and the inverters feed the DN system with associated loads. The current of the inverter (LV side of 400V/20kV transformer) is shown in Fig. 12, wherein the inrush current is limited within the inverter's output capacity. The results show that the inverter system is capable of handling the inrush current and at the same time also feeding loads in the grid. The inrush peak starts to develop after closing the CB but there is a rapid reduction of the current once the inverter starts to react. The event is terminated in less than 20ms, and a typical recurring and decaying phenomenon of inrush peak is not occurring in the system.

Also, voltage and current on the MV side are illustrated in Fig. 13 which are recorded by a relay. It is evident that by energizing the MV grid, inrush current is drawn from the

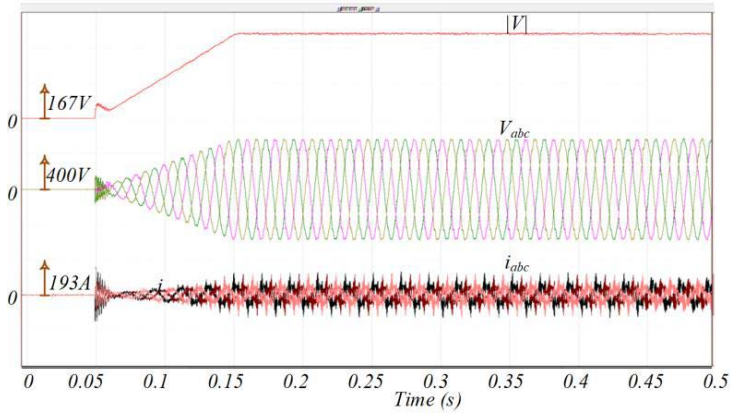

FIGURE 11. Experimental results of control scheme with voltage reference modifier in the outer loop: PCC voltage and inverter current, voltage.

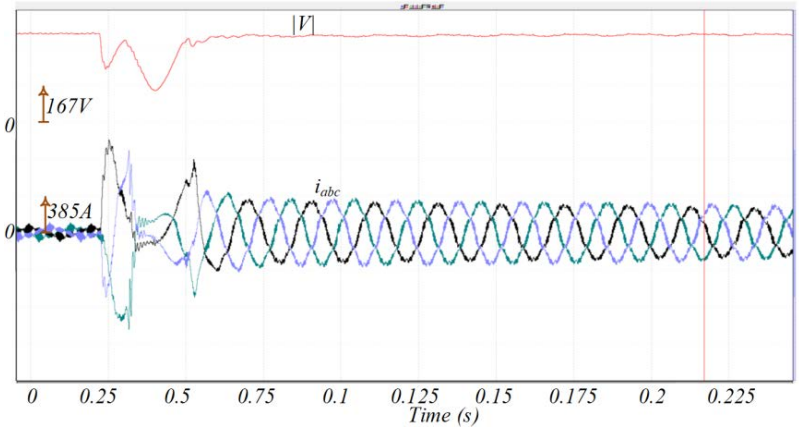

FIGURE 12. Experimental results of control scheme with current reference modifier in voltage loop. a) Inverter output voltage b) Inverter output current.

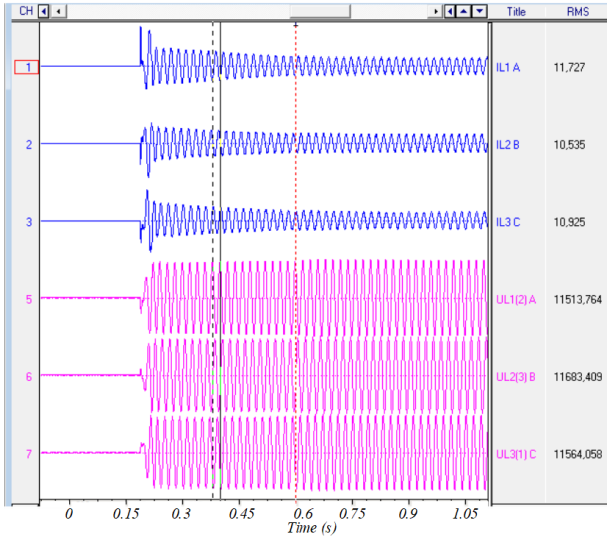

FIGURE 13. Experimental results of control scheme with current reference modifier in voltage loop. MV bus voltage: UL1 (2)A, UL1 (3)B, UL1(1) C. MV bus current: IL1 A, IL3 B, IL3 C.

inverter which is caused by 20kV/400V transformers. Two points should be mentioned about these results, 1) the inrush current in MV side is limited to the rated current of line and is under control, 2) MV voltage reaches its nominal in less than half cycle and then is fixed. Therefore, it can be concluded that the proposed method is efficiently able to feed the MV grid with standard voltage and control the inrush current.

In summary, the presented experimental results show that the proposed control scheme with the reference modifier in voltage loop has a promising performance in limitation of sympathetic inrush current without the need to consider transformers parameters, the timing of circuit breaker and MV distribution system structure.

V. CONCLUSION

In this paper, two control schemes have been designed and implemented for an inverter-based battery storage system to perform the black start of island operated medium voltage distribution network. The cascaded approach, with an outer droop loop (voltage reference generator) as well as an inner loop including voltage and current loops, was used to develop control schemes. A reference modifier was added either to the outer loop or the voltage loop in order to limit transformers' inrush currents. The control scheme performance was tested through energization of real 20 kV distribution by 1 MVA battery energy storage. The obtained results verified that the control scheme with reference modifier in the voltage loop is able to feed the MV grid with a good performance wherein the

grid was fed with the nominal voltage and the inverter current is the maximum current. The proposed control scheme mitigates peaking and decaying characteristics of typical inrush current. This leads to a reduction in the inverter rating as well as the cost because oversizing caused by inrush current is not needed.

REFERENCES

[1] J. Kumar, C. Parthasarathy, M. Västi, H. Laaksonen, M. Shafie-Khah, and K. Kauhaniemi, "Sizing and allocation of battery energy storage systems in Åland islands for large-scale integration of renewables and electric ferry charging stations," *Energies*, vol. 13, no. 2, p. 317, Jan. 2020, doi: 10.3390/en13020317.

[2] H. Jain, G.-S. Seo, E. Lockhart, V. Gevorgian, and B. Kroposki, "Black-start of power grids with inverter-based resources," in *Proc. IEEE Power Energy Soc. Gen. Meeting (PESGM)*, Aug. 2020, pp. 1–5, doi: 10.1109/PESGM41954.2020.9281851.

[3] National Grid ESO. (Jun. 2019). *Black Start From Non-Traditional Generation Technologies*. [Online]. Available: https://www.nationalgrideso.com/document/148201/download

[4] J. M. Guerrero, J. C. Vásquez, J. Matas, M. Castilla, and L. G. de Vicuña, "Control strategy for flexible microgrid based on parallel line-interactive UPS systems," *IEEE Trans. Ind. Electron.*, vol. 56, no. 3, pp. 726–736, Mar. 2009, doi: 10.1109/TIE.2008.2009274.

[5] M. Shahparasti, M. Savaghebi, E. Adabi, and T. Ebel, "Dual-input photovoltaic system based on parallel Z-source inverters," *Designs*, vol. 4, no. 4, pp. 1–16, 2020, doi: 10.3390/designs4040051.

[6] I. Agirman and V. Blasko, "A novel control method of a VCS without AC line voltage sensors," *IEEE Trans. Ind. Appl.*, vol. 39, no. 2, pp. 519–524, Mar. 2003, doi: 10.1109/TIA.2003.808925.

[7] *Recommended Practice and Requirements for Harmonic Control in Electric Power Systems*, Standard IEEE 519-2014, IEEE Power and Energy Society, 2014.

[8] A. M. Roslan, K. H. Ahmed, S. J. Finney, and B. W. Williams, "Improved instantaneous average current-sharing control scheme for parallel-connected inverter considering line impedance impact in microgrid networks," *IEEE Trans. Power Electron.*, vol. 26, no. 3, pp. 702–716, Mar. 2011, doi: 10.1109/TPEL.2010.2102775.

[9] R. Heyderi, M. Alhashem, S. Peyghami, T. Dragicevic, and F. Blaabjerg, "Unified power sharing control in hybrid AC/DC microgrids employing synchronous machine principle," in *Proc. 20th Eur. Conf. Power Electron. Appl. (EPE ECCE Europe)*, 2018, pp. P.1–P.8.

[10] L. Hang, S. Liu, G. Yan, B. Qu, and Z.-Y. Lu, "An improved deadbeat scheme with fuzzy controller for the grid-side three-phase PWM boost rectifier," *IEEE Trans. Power Electron.*, vol. 26, no. 4, pp. 1184–1191, Apr. 2011, doi: 10.1109/TPEL.2010.2089645.

[11] M. Pichan and H. Rastegar, "Sliding-mode control of four-leg inverter with fixed switching frequency for uninterruptible power supply applications," *IEEE Trans. Ind. Electron.*, vol. 64, no. 8, pp. 6805–6814, Aug. 2017, doi: 10.1109/TIE.2017.2686346.

[12] M. Shahparasti, R. Heydari, M. Savaghebi, J. Rodriguez, and F. Blaabjerg, "Hybrid four-wire three-level inverter equipped with model predictive control for UPS applications," in *Proc. IEEE 21st Workshop Control Modeling Power Electron. (COMPEL)*, Nov. 2020, pp. 4–8.

[13] M. Shahparasti, M. Mohamadian, A. Yazdian, A. A. Ahmad, and M. Amini, "Derivation of a stationary-frame single-loop controller for three-phase standalone inverter supplying nonlinear loads," *IEEE Trans. Power Electron.*, vol. 29, no. 9, pp. 5063–5071, Sep. 2014. [Online]. Available: http://ieeexplore.ieee.org/xpls/abs_all.jsp?arnumber=6651854

[14] M. H. Marzebali, M. Mazidi, and M. Mohiti, "An adaptive droop-based control strategy for fuel cell-battery hybrid energy storage system to support primary frequency in stand-alone microgrids," *J. Energy Storage*, vol. 27, Feb. 2020, Art. no. 101127, doi: 10.1016/j.est.2019.101127.

[15] J. M. Guerrero, J. Matas, L. G. de Vicuña, M. Castilla, and J. Miret, "Wireless-control strategy for parallel operation of distributed-generation inverters," *IEEE Trans. Ind. Electron.*, vol. 53, no. 5, pp. 1461–1470, Oct. 2006, doi: 10.1109/TIE.2006.882015.

[16] H. Dashti, M. Davarpanah, M. Sanaye-Pasand, and H. Lesani, "Discriminating transformer large inrush currents from fault currents," *Int. J. Electr. Power Energy Syst.*, vol. 75, pp. 74–82, Feb. 2016, doi: 10.1016/j.ijepes.2015.08.025.

[17] S. Schramm, C. Sihler, and S. Rosado, "Limiting sympathetic interaction 517 between transformers caused by inrush transients," *Int. Conf. Power Syst. Transients (IPST2011)*. Delft, The Netherlands, Jun. 2011, pp. 1–6.

[18] J. Mitra, X. Xu, and M. Benidris, "Reduction of three-phase transformer inrush currents using controlled switching," *IEEE Trans. Ind. Appl.*, vol. 56, no. 1, pp. 890–897, Jan. 2020, doi: 10.1109/TIA.2019.2955627.

[19] A. Yahiou, A. Bayadi, and B. Babes, "Mitigation of sympathetic inrush current in transformer using the technique of point on voltage wave control switching," in *Proc. Int. Conf. Commun. Electr. Eng. (ICCEE)*, Dec. 2018, pp. 1–6, doi: 10.1109/CCEE.2018.8634501.

[20] N. Mohan and T. M. Undeland, *Power Electronics: Converters, Applications, and Design*. Hoboken, NJ, USA: Wiley, 2007.

[21] M. Shahparasti, P. Catalan, I. Garcia, J. Ignacio Candela, A. Tarraso, and A. Luna, "Enhanced performance controller for high power wind converters connected to weak grids," *IET Renew. Power Gener.*, vol. 14, no. 12, pp. 2058–2067, Sep. 2020, doi: 10.1049/iet-rpg.2019.1021.

[22] M. Shahparasti, P. Catalán, J. I. Candela, A. Luna, and P. Rodríguez, "Advanced control of a high power converter connected to a weak grid," in *Proc. IEEE Energy Convers. Congr. Expo. (ECCE)*, Milwaukee, WI, USA, Sep. 2016, pp. 1–7.

[23] Z. Spoljaric, V. Jerkovic, and M. Stojkov, "Measurement system for transformer inrush current higher harmonics determination," in *Proc. 23rd DAAAM Int. Symp. Intell. Manuf. Autom.*, 2012, vol. 2, no. 1, pp. 617–622, doi: 10.2507/23rd.daaam.proceedings.145.

[24] T. Specht, "Transformer inrush and rectifier transient currents," *IEEE Trans. Power App. Syst.*, vol. PAS-88, no. 4, pp. 269–276, Apr. 1969.

[25] M. Shahparasti, J. Rocabert, R. S. Munoz, A. Luna, and P. Rodriguez, "Smart AC storage based on microbial electrosynthesis stack," in *Proc. 7th Int. Conf. Renew. Energy Res. Appl. (ICRERA)*, Oct. 2018, pp. 1086–1091, doi: 10.1109/ICRERA.2018.8566904.

[26] R. Heydari, T. Dragicevic, and F. Blaabjerg, "High-bandwidth secondary voltage and frequency control of VSC-based AC microgrid," *IEEE Trans. Power Electron.*, vol. 34, no. 11, pp. 11320–11331, Nov. 2019, doi: 10.1109/TPEL.2019.2896955.

[27] B. Wei, A. Marzabal, R. Ruiz, J. M. Guerrero, and J. C. Vasquez, "DAVIC: A new distributed adaptive virtual impedance control for parallel-connected voltage source inverters in modular UPS system," *IEEE Trans. Power Electron.*, vol. 34, no. 6, pp. 5953–5968, Jun. 2019, doi: 10.1109/TPEL.2018.2869870.

[28] M. Shahparasti, P. Catalán, N. Roslan, J. Rocabert, R.-S. Muñoz-Aguilar, and A. Luna, "Enhanced control for improving the operation of grid-connected power converters under faulty and saturated conditions," *Energies*, vol. 11, no. 3, p. 525, Feb. 2018, doi: 10.3390/en11030525.

[29] S. B. Naderi, M. Negnevitsky, A. Jalilian, and M. T. Hagh, "Efficient fault ride-through scheme for three phase voltage source inverter-interfaced distributed generation using DC link adjustable resistive type fault current limiter," *Renew. Energy*, vol. 92, pp. 484–498, Jul. 2016, doi: 10.1016/j.renene.2016.02.016.

[30] M. Shahparasti, P. Catalán, N. Roslan, J. Rocabert, R.-S. Muñoz-Aguilar, and A. Luna, "Enhanced control for improving the operation of grid-connected power converters under faulty and saturated conditions," *Energies*, vol. 11, no. 3, p. 525, Feb. 2018, doi: 10.3390/en11030525.

[31] *Voltage Characteristics of Electricity Supplied by Public Electricity Networks*, Standard EN 50160, CENELEC, 2010.

MAHDI SHAHPARASTI (Senior Member, IEEE) received the M.Sc. and Ph.D. degrees (Hons.) in electrical engineering from Tarbiat Modares University, Tehran, Iran, in 2010 and 2014, respectively. From 2010 to 2014 and from 2016 to 2017, he was a Research and Development Engineer with JDEVS Company in designing power converters for UPS, motor drive, and hybrid energy systems. In 2015 and from 2017 to 2019, he was with the Technical University of Catalonia, respectively, as a Postdoctoral Researcher in controlling high-power grid-connected converters with Ingeteam Company and a two-year Marie Skłodowska-Curie Postdoctoral Fellow in developing interlinking converters for power-to-gas plants. Then, he was with the University of Southern Denmark in developing the hardware and control of dc/dc and dc/ac converters in the period 2019–2021. He is currently an Assistant Professor of power electronics at the University of Vaasa, Finland. His research interests include hardware design, control, stability and dynamic analysis of power electronic systems, power quality, microgrids, renewable energy resources, and motor drive systems.

HANNU LAAKSONEN (Member, IEEE) received the M.Sc. (Tech.) degree in electrical power engineering from the Tampere University of Technology, Tampere, Finland, in 2004, and the Ph.D. (Tech.) degree in electrical engineering from the University of Vaasa, Vaasa, Finland, in 2011. His employment experience includes working as a Research Scientist at VTT Technical Research Centre of Finland and the University of Vaasa. He has previously worked as a Principal Engineer at ABB Ltd., Vaasa. He is currently a Professor of electrical engineering at the University of Vaasa. He is also a Manager of the Smart Energy Master's Program. His research interests include the protection of low-inertia power systems (including microgrids), active management of distributed and flexible energy resources in future smart energy systems, future-proof technology, and market concepts for smart grids.

KIMMO KAUHANIEMI (Member, IEEE) received the M.S. and Ph.D. degrees in electrical engineering from the Tampere University of Technology, Finland, in 1987 and 1993, respectively. Previously, he was employed by ABB Corporate Research and VTT Technical Research Centre of Finland. He is currently with the University of Vaasa, where he is a Professor of electrical engineering and leads the Smart Electric Systems Research Group. His research interests include the power system transient simulation, protection of power systems, grid integration of distributed generation, and microgrids.

PANU LAUTTAMUS received the M.Sc. and Ph.D. degrees in power electronics from the Tampere University of Technology, Finland, in 2006 and 2014, respectively. He has been with Danfoss Drives, since 2012, to develop industrial power electronic converters and ac drives. His research interests include intelligent ac/dc and dc/dc converters for electrification and decarbonization.

JAN STRANDBERG received the M.Sc. (Tech.) degree in electronics and electrical engineering from the Aalto University School of Electrical Engineering, Espoo, Finland, in 2016. He has been working in power distribution at DSO level at Fortum and Caruna, since 2012. His employment experiences include working in network planning and network operations and also projects, including distributed generation and battery storages.